Available online at www.sciencedirect.com
SCIENCE DIRECT®
Vibrational Spectroscopy 33 (2003) 83–92
VIBRATIONAL SPECTROSCOPY
www.elsevier.com/locate/vibspec

Vibrational and quantum-chemical study of pH dependent molecular structures of (hydroxypyridin-4-yl-methyl)phosphonic acid

Małgorzata Barańska[a], Katarzyna Chruszcz[a], Kamilla Małek, Joanna Kulinowska[a], Leonard M. Proniewicz[a,b,*]

[a]*Faculty of Chemistry, Jagiellonian University, 3 Ingardena Str., 30-060 Kraków, Poland*
[b]*Laser Raman Laboratory, Regional Laboratory of Physicochemical Analysis and Structural Research, Jagiellonian University, 3 Ingardena Str., 30-060 Kraków, Poland*

Received 15 May 2003; received in revised form 2 July 2003; accepted 2 July 2003

Abstract

Vibrational study of pH dependent molecular structures of (hydroxypyridin-4-yl-methyl)phosphonic acid is discussed based on experimental data and quantum-chemical calculations. A cationic, a zwitteranionic as well as mono- and dianionic forms of the acid are considered in our work. Equilibrium geometries, harmonic vibrational frequencies were calculated for all species of (hydroxypyridin-4-yl-methyl)phosphonic acid deprotonated in different way by using DFT (B3PW91) with 6-31G(d,p) basis set. The computed properties are compared to the experimental values. Additionally, charge distributions and aromaticity index were calculated for species studied here by using generalized atomic polar tensor (GAPT) and harmonic oscillator model of aromaticity (HOMA), respectively.

Keywords: (Hydroxypyridin-4-yl-methyl)phosphonic acid; FT-IR; FT-Raman; Quantum-chemical calculation; DFT; GAPT; HOMA

1. Introduction

In recent years sodium salts of some bisphosphonates have been widely used in the treatment of osteolitic bone disease in humans. The pharmacological function of these compounds is connected with their relatively stable C–P bonds. Moreover, they are totally resistant to enzymatic hydrolysis. The powerful bisphosphonate, 2-(3-pyridinyl)-1-hydroxyethylidene bisphosphonic acid (so-called risedronate) has been found to be efficient even at the single intravenous dose [1]. As can be expected, structural modification of the bisphosphonates can lead to considerable variation in their physicochemical, biological, therapeutic and toxicological properties [2–7].

The class of phosphonopyridine derivatives has been extensively investigated by our group [8–12]. One of them, (hydroxypyridin-4-yl-methyl)phosphonic acid (MC4) is studied in this work. We report the dependence of the ligand structures on pH measured by spectroscopic methods and supported by quantum-chemical calculations. Until now, FT-IR and FT-Raman spectra of (hydroxypyridin-4-yl-methyl)phosphonic

* Corresponding author. Tel.: +48-12-633-63-77x2253; fax: +48-12-634-05-15.
E-mail addresses: baranska@chemia.uj.edu.pl (M. Barańska), proniewi@chemia.uj.edu.pl (L.M. Proniewicz).

0924-2031/$ – see front matter
doi:10.1016/S0924-2031(03)00092-4

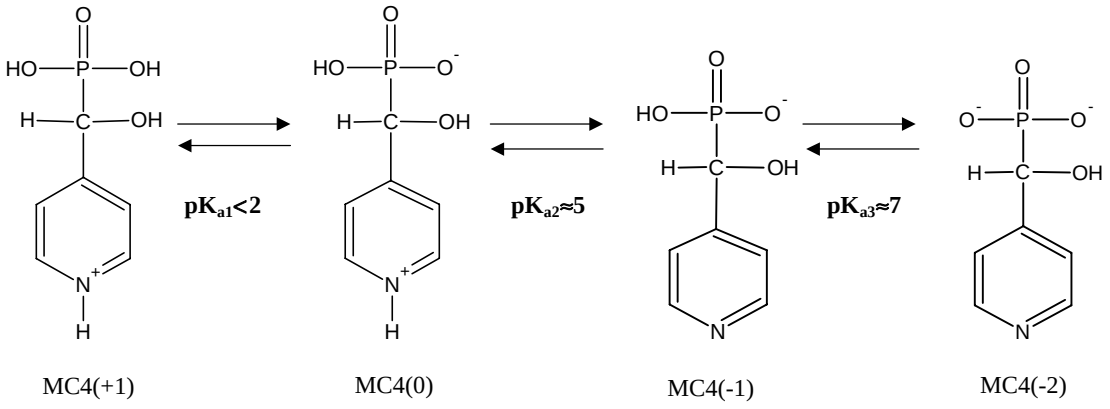

Fig. 1. (Hydroxy-pyridin-4-yl-methyl)phosphonic acid (MC4) species in aqueous solution.

acid and the assignment of their vibrational patterns have not been reported yet.

Up to four species are expected for MC4 that are pH dependent in aqueous solution [7,9]. Their structures are shown in Fig. 1. The exact pK_a values were calculated from potentiometric data for two structural isomers of MC4 with a substituent –CHOH–PO_3H_2 in positions *ortho* and *meta* of the pyridine ring [7]. Potentiometric data of MC4 have not been reported thus far. Potentiometric data have showed the presence of two labile protons within the experimentally measurable pH range (2.0–12.0). However, one more deprotonation is postulated at pH below 2.0. This is supported by our NMR measurements and quantum-chemical calculations of (hydroxypyridin-3-yl-methyl)phosphonic acid in D_2O solution in p*D* range of 1.5–9.0 [9].

Based on previous potentiometric studies on *ortho*- and *meta*-isomers of MC4 we proposed the existence of four MC4 species (cf. Fig. 1). They are formed after the consecutive deprotonation caused by increasing of pH of solution in accordance with our earlier studies [7,9]. The pK_{a1} corresponds to the dissociation of one of the phosphonic protons and it usually occurs below 2.0 [2,5,7]. The next protonation constants, pK_{a2} and pK_{a3}, are related to proton of the pyridine nitrogen atom and the second proton of the phosphonic group, respectively. Their values were established to 5.10 and 5.24 (pK_{a2}) and 7.25 and 6.93 (pK_{a3}) for aforementioned isomers of MC4. Based on these data we postulate similar protonation constant values for MC4.

In this work, we report a theoretical study for all possible MC4 molecular forms presented in Fig. 1. We also discuss their geometrical parameters, aromaticity (index harmonic oscillator model of aromaticity, HOMA) and charge distribution using generalized atomic polar tensors (GAPT) method. To give a detailed description of the calculated and the observed vibrational modes, normal coordinate analysis calculation (potential energy distribution, PED) were also performed.

2. Experimental

2.1. Compound

The title compound (MC4) was synthesized as described earlier [13,14] and obtained in zwitteranionic form. Titration of MC4 aqueous solutions with sodium hydroxide allowed to obtain its anionic form. Dianion of MC4 (disodium salt) was precipitated at pH 8.0.

2.2. Spectral measurements

For FT-Raman measurements, a few milligrams of MC4 were placed in a glass capillary and measured directly (180° geometry). Five hundred twelve scans were collected with resolution of 4 cm^{-1}. FT-IR spectra were run in KBr discs by using standard procedures of sample preparation for these measurements. One hundred twenty-eight scans with resolution of 2 cm^{-1} were accommodated for FT-IR spectra.

FT-Raman spectra were recorded on a BIO-RAD step-scan spectrometer model FTS 6000 combined with

a BIO-RAD model FTS 40 Raman Accessory. Excitation at 1064 nm was effected by a SPECTRA-PHYSICS model TOPAZ T10-106c cw Nd:YAG laser. Power at the sample was maintained at 200 mW. FT-IR spectra were measured on a BRUKER spectrometer model EQUINOX55 equipped with GLOBAR excitation source and TGS detector. Frequency accuracy is estimated as $\pm 1\ cm^{-1}$.

2.3. Calculations

The geometry optimisation and vibrational frequencies of four MC4 species were performed using quantum-chemical calculations. Additionally, GAPT [15] and aromaticity index HOMA [16,17] were calculated.

All calculations were carried out at density functional theory (DFT) level using the B3PW91 [18–20] exchange-correlation functional implemented in Gaussian'98 program [21]. This method is recommended by Scott and Radom [22] and gives the best agreement between experimental and calculated frequencies. All calculation were performed with 6-31G** basis set where the polarization functions allow better descriptions of polar bonds of hydroxylate and phosphonate groups in molecules.

Program GAR2PED [23] was used for GAPT calculation and potential energy distribution. PED provides quantification of the contribution of internal coordinate to a normal coordinate [24,25]. For that purpose, the contribution of the diagonal force constant of internal coordinate to the vibrational eigenvalue is expressed as a percentage. Vibrational analysis of frequency modes was performed by graphical user interface MOLEKEL [26].

Calculations were performed assuming C_1 point group symmetry for all studied species of MC4. The computed frequencies were scaled by empirical factor of 0.9573 [22] to correct incomplete incorporation of electron correlation and the use of finite basis set.

3. Results and discussion

3.1. Structural study

The comparison of the optimised bond lengths and angles for all discussed MC4 forms is presented in Table 1. It can be noticed that the MC4(0) bond distances for following pairs: N_1–C_2 and N_1–C_6, C_2–C_3 and C_6–C_5, C_3–C_4 and C_4–C_5 are almost equal and very close to counterparts of the pyridine ring. The C–H lengths of this MC4 form are in the range 1.082–1.084 Å, comparable to the related pyridine bonds. Also, some elongation of MC4 molecule along the vertical plane going from N_1 to C_4 atoms is observed.

Table 1
Calculated length bonds (Å) of MC4 species

Bonds and angles	MC4(+1)	MC4(0)	MC4(−1)	MC4(−2)
N_1–C_2	1.288	1.359	1.341	1.350
N_1–C_6	1.408	1.356	1.337	1.345
C_2–C_3	1.343	1.367	1.389	1.383
C_3–C_4	1.347	1.416	1.402	1.415
C_4–C_5	1.346	1.412	1.396	1.411
C_4–C_7	1.514	1.453	1.497	1.455
C_5–C_6	1.341	1.369	1.392	1.387
N_1–H_{20}	0.995	1.010	–	–
C_2–H_{13}	1.103	1.083	1.091	1.095
C_3–H_{14}	1.103	1.084	1.087	1.088
C_5–H_{15}	1.103	1.082	1.084	1.086
C_6–H_{16}	1.103	1.084	1.092	1.096
C_7–O_8	1.404	1.399	1.418	1.412
C_7–P_9	1.795	1.948	1.884	2.023
C_7–H_{17}	1.114	1.099	1.104	1.103
O_8–H_{18}	0.942	0.970	0.971	1.014
P_9–O_{10}	1.683	1.669	1.705	1.561
P_9–O_{11}	1.601	1.496	1.502	1.530
P_9–O_{12}	1.682	1.497	1.504	1.523
O_{10}–H_{19}	0.941	0.967	0.967	–
O_{12}–H_{21}	0.94	–	–	–

As expected, the consecutive MC4 proton dissociation influences structural parameters of the species obtained in solid state at different pH. Deprotonation of the pyridine nitrogen causes shortening of both N_1–C_2 and N_1–C_6 bonds and concomitant lengthening of the adjacent bonds, i.e. C_2–C_3 and C_5–C_6 (for the atom numbering see Fig. 2). On the other hand, both protons that dissociate from the phosphonic group do not have significant impact on pyridine ring bonds since this group is not directly attached to the ring. But this deprotonation causes fairly significant shortening of P_9–O_{12} (first deprotonation, 1.682 Å in MC4(+1) to 1.497 Å in MC4(0)) and P_9–O_{10} (third deprotonation, 1.705 Å in MC4(−1) to 1.561 Å in MC4(−2)) bonds. It is due to partial delocalisation of π-electrons in the $-PO_3^{2-}$ group. The same behaviour has been reported earlier [11] for structural isomers of MC4.

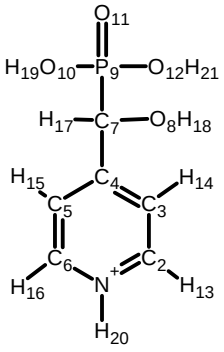

Fig. 2. The atom numbering of MC4.

The deprotonation of the pyridine nitrogen influences mainly dihedral angles in which this atom is involved, i.e. N_1–C_2–C_3 and N_1–C_6–C_5 (data not presented in Table 1). It is worth noting that the phosphonic proton dissociation results in decreasing C_7–O_8–H_{18} angle and brings the hydroxyl proton closer to the phosphonic group.

3.2. Aromaticity

Study of MC4 species in aqueous solution at different pH has proved that this acid is H-bond donor or acceptor depending upon pH. Additionally, deprotonation or protonation of either phosphonic group or the pyridine nitrogen atom influences π-electronic system of the ring. In the present work, we determine the dependence of the consecutive MC4 deprotonation, including also the side chain, on the ring aromaticity. So far, the aromaticity of pyridine has been well documented [27,28], but there is no information on its phosphonosubstituted ring.

The aromaticity of MC4 has been studied in this work on the basis of quantum-chemical data obtained by using B3PW91/6-31G** method. The harmonic oscillator model of aromacity index, that gives quantitative estimation of heteroring aromaticity, was calculated for the cation, the zwitteranion and two anions of MC4.

Index HOMA is based on structural criterion and depends strongly on terms called GEO and EN (HOMA = 1 − EN − GEO) [16,17]. The term GEO describes the decrease of aromatization due to the increase of the bond length variation, whereas the term EN shows, how far the mean bond lengths deviate from the optimal bond length. In other words, GEO is a function of the bond length fluctuation, while EN characterizes the decrease of the ring stability due to bond elongation. The EN and GEO terms are not correlated with each other. The successful application of index HOMA for pyridine molecule and its derivatives confirms the usefulness of this method. Thus, a neat pyridine HOMA = 0.998 (EN = −0.009, GEO = 0.011) [29].

In this work, we calculated aromaticity of all four MC4 species that exist in aqueous solution at different pH (Fig. 1). Obtained results are presented in Fig. 3 as a graph with EN and GEO values collected in the table. The calculated aromaticity index HOMA for unsubstituted pyridine and its cation are also listed. The obtained value of 0.995 for pyridine is in very good agreement with data cited above and confirms the correctness of conducted calculations. It is noteworthy that deprotonation of pyridine increases the ring aromaticity as was reported earlier [11].

The investigated species of MC4 show high aromaticity with the index HOMA above 0.93 except the MC4(0) zwitteranion (HOMA = 0.89). The highest values (0.96–0.99) were obtained for the MC4(+1) cation and the MC4(−1) monoanion. Surprisingly, deprotonation of the phosphonic group decreases the index HOMA. On the other hand, proton dissociation from the pyridine nitrogen results in the increase of MC4 aromaticity similarly to that observed for unsubstituted pyridine. The MC4(0) zwitteranion is characterized by the largest GEO term which may be explained by elongation of C_3–C_4 and C_4–C_5 bonds.

Similar correlation between the consecutive deprotonation and the pyridine ring aromaticity is observed for structural isomer of MC4 with the substituent in *meta*-position [11]. The index HOMA obtained for both studied isomers are almost equal with only one difference related to the aromaticity of zwitteranions. However, based on our theoretical results, we conclude that the position of pyridine substitution does not significantly influence the ring aromaticity.

3.3. Generalized atomic polar tensors

The knowledge of atomic charge distributions is essential for the interpretation of molecular properties. So far, several procedures to atomic charges analysis have been proposed, e.g. Mulliken approach [30,31],

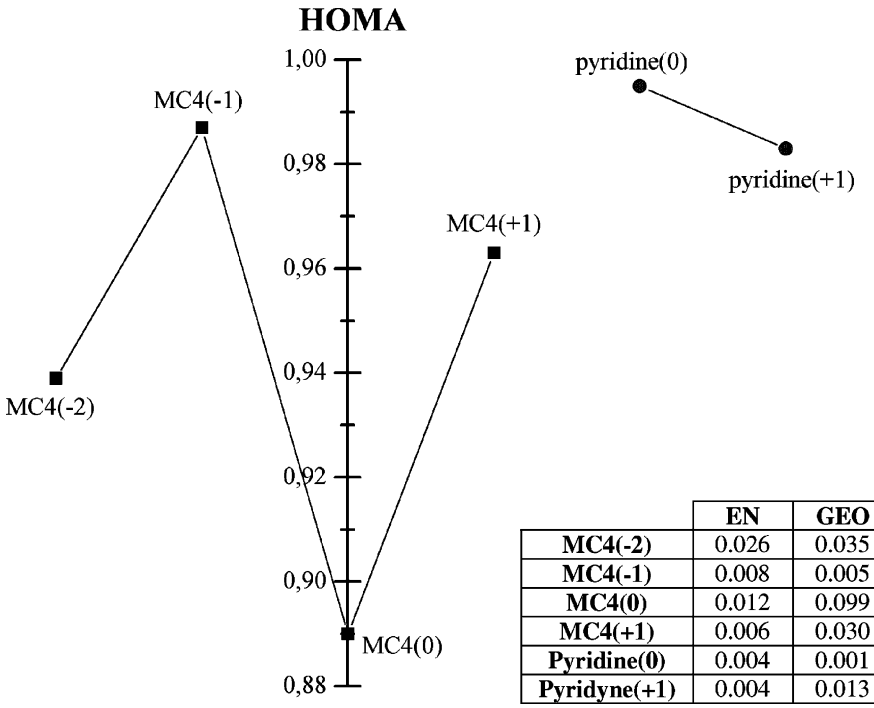

	EN	GEO	HOMA
MC4(-2)	0.026	0.035	0.939
MC4(-1)	0.008	0.005	0.987
MC4(0)	0.012	0.099	0.890
MC4(+1)	0.006	0.030	0.963
Pyridine(0)	0.004	0.001	0.995
Pyridyne(+1)	0.004	0.013	0.983

Fig. 3. The aromaticity index HOMA for MC4 species in aqueous solution.

Lödwin approach [32], natural population analysis of Reed et al. [33], atomic polar tensor [34] or generalized atomic polar tensor by Ciosłowski [15]. Unfortunately, there is no one arbitrary algorithm for estimating atomic charges despite the fact that methods have been derived from the molecular orbital calculations.

In this work, the GAPT analysis for calculation of atomic charges was used. GAPT is correlated with the APT analysis [34], which is composed from derivatives of the molecular dipole moment with respect to the Cartesian coordinates of any atom in the molecule. The GAPT charge of an atom is defined as one third of the trace of APT. This approach has the following advantages: (1) the atomic charges are invariant with respect to rotations and translations of the molecule; (2) partial atomic charges sum up to the total electric charges of the molecule; (3) this reflects the symmetry of the molecule; (4) has a clear physical meaning; (5) is not dependent upon the choice of a particular basis set [15]. It should be stressed out that Mulliken population analysis implemented in Gaussian'98 program is incorrect for species bearing some ionic character. This ''classical'' method of the electron distribution analysis yields atomic charges on separate atoms that reflect mostly properties of the basis set used in calculations rather than distribution itself. It was the reason for the application more reliable tool, i.e. the GAPT atomic charges calculated by GAR2PED program.

Table 2 presents the atomic charges of pH dependent MC4 species calculated by using B3PW91/6-31G** method. All obtained molecular structures show negative partial charges on the nitrogen atoms and positive charges on *ortho*- and *para*-carbon atoms analogously to that observed for unsubstituted pyridine [29]. The deprotonation of the pyridine nitrogen decreases C_2, C_4 and C_6 partial charges, whereas the second dissociation from the phosphonic group results in increase of these charges. On the other hand, negatively charged C_3 and C_5 show opposite behaviour. They become less negative after the nitrogen deprotonation (MC4(−1)) and more negative after phosphonic protons dissociations (MC4(−2)).

As has been calculated for all MC4 forms, significant charge changes of the phosphorus atom are not

Table 2
Generalized atomic polar tensors (GAPT) of MC4 species

Atom	MC4(+1)	MC4(0)	MC4(−1)	MC4(−2)
N_1	−0.296	−0.473	−0.511	−0.759
C_2	0.235	0.328	0.265	0.393
C_3	−0.207	−0.255	−0.197	−0.279
C_4	0.409	0.568	0.285	0.555
C_5	−0.221	−0.278	−0.194	−0.316
C_6	0.238	0.333	0.264	0.412
C_7	0.060	−0.322	0.038	−0.411
O_8	−0.598	−0.588	−0.659	−0.716
P_9	2.002	1.943	1.853	1.961
O_{10}	−0.895	−0.911	−0.912	−1.153
O_{11}	−0.819	−0.859	−0.924	−1.029
O_{12}	−0.816	−0.878	−0.894	−0.931
H_{13}	0.119	0.083	−0.028	−0.077
H_{14}	0.145	0.119	0.090	0.044
H_{15}	0.144	0.107	0.062	0.032
H_{16}	0.115	0.076	−0.040	−0.093
H_{17}	−0.001	0.038	−0.076	−0.07
H_{18}	0.344	0.343	0.326	0.405
H_{19}	0.365	0.279	0.253	–
H_{20}	0.312	0.285	–	–
H_{21}	0.365	–	–	–

observed. They vary from 1.853 (MC4(−1)) to 2.002 (MC4(+1)) (Table 2). Similar observation was made for the structural isomer of MC4 with the substituent in *meta*-position [11]. Continuous increase of negative charge is however observed for oxygen atoms of the phosphonic group during the consecutive steps of deprotonation. As expected, the most negative charges appear on oxygen atoms of the phosphonic group in MC4(−2). Moreover, O_8 is less negatively charged than oxygen atoms of the phosphonic group, i.e. O_{10}–O_{12}. This is probably due to the polarisation effect of the C–O bond in comparison to P–O bonds as well as differences in bond lengths (the C–O bond is shorter than P–O).

The direction of discussed changes of charge distribution seems to follow the aromaticity changes estimated by the HOMA index (see Fig. 2 and the paragraph above).

3.4. Vibrational study

Experimental vibrational spectra in solid state MC4(0) and MC4(−2) (precipitated from aqueous solution at pH 8.0) are presented in Fig. 4 (FT-IR) and Fig. 5 (FT-Raman). The upper spectra show MC4(0) as the zwitteranion whereas the bottom represents the MC4(−2) dianion. The calculated and experimental vibrational frequencies and the proposed assignments are summarized in Tables 3 and

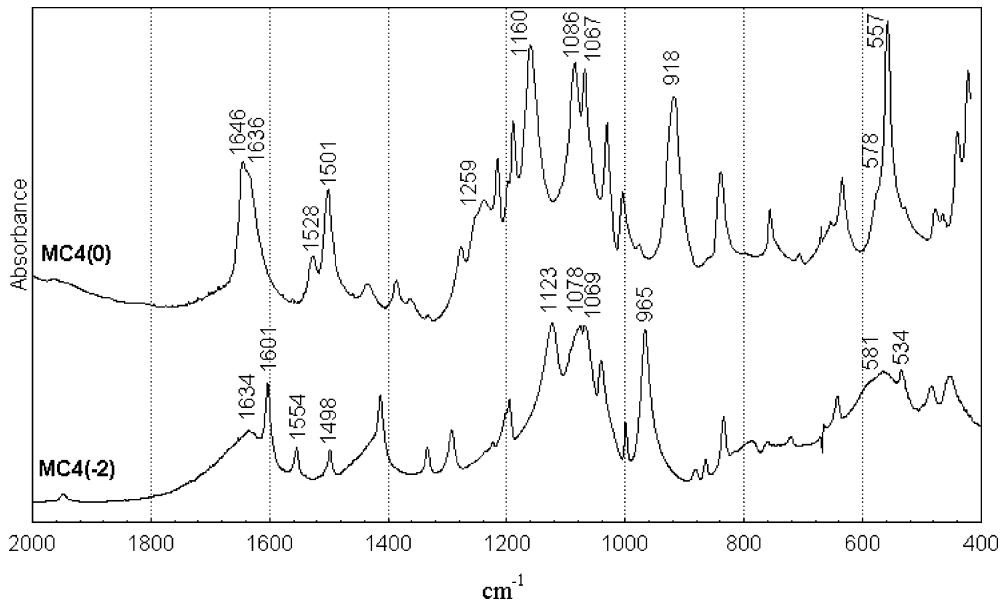

Fig. 4. FT-IR spectra of zwitteranion MC4(0) and dianion MC4(−2) in solid state precipitated from aqueous solution at the pH values 3.0 and 8.0, respectively.

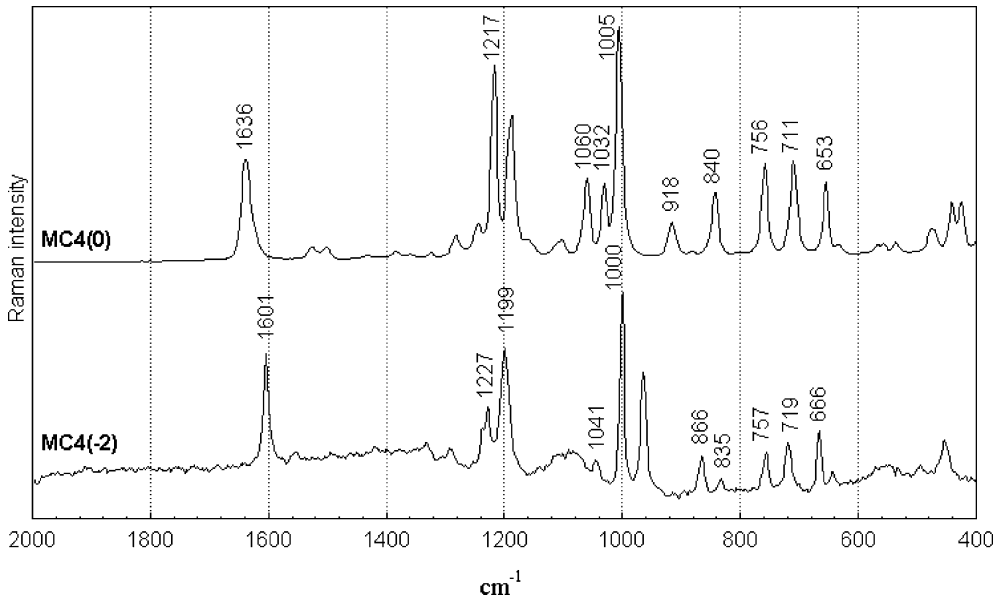

Fig. 5. FT-Raman spectra of zwitteranion MC4(0) and dianion MC4(−2) in solid state precipitated from aqueous solution at the pH values 3.0 and 8.0, respectively.

4. Potential energy distribution of normal coordinates presented in Tables 3 and 4 are shown in the range 2000–400 cm^{-1} only, since the frequency region above 2000 cm^{-1} is not very important for the structure discussion. Some changes seen in the spectra are due to hydrogen bonds formation. However, in our quantum-chemical calculations isolated molecules were applied in the first round of structure modelling, because of neglect of hydrogen bond effect. Besides the strong impact of H-bonds is observed in the high frequency range of the spectra only (not showed).

Generally, spectra of both presented MC4 species show some similarities such as several well-documented features associated with characteristic pyridine ring and phosphonic group vibrations. These experimental modes are clearly assigned in Tables 3 and 4 and there is no need to discuss them one by one. The most characteristic vibrations of pyridine ring are observed at 1646, 1636 and 1528 cm^{-1} for MC4(0) and 1634 and 1601 cm^{-1} for MC5(−2). It has to be noted that sometimes a slight change in band frequency on going from MC4(0) to MC4(−2) appears to be a mode of different PED. This is obviously due to structural changes caused by proton dissociation. For example, the 1636 cm^{-1} vibration, as revealed by PED, is mainly due to the $\delta(N_1–H)$ vibration (30%) when after deprotonation of the pyridine nitrogen this mode disappears. Instead the 1605 cm^{-1} band appears (MC4(−2)) with PED, as has to be expected drastically different.

Our special attention is to characterize modes that are associated with the phosphonic group vibrations. Phosphonic acids in ionic forms can be characterized by the P=O stretching, ν(P=O), (P^{---}O) stretching, ν(P^{---}O), P–O(H) stretching, ν(P–O), and P–C stretching, ν(P–C), vibrations. In many cases, ring or aliphatic chain stretching and deformation vibrations may easily obscure bands that are associated with stretchings listed above. Additionally, in the presence of strong hydrogen bonds often encountered in these compounds, ν(P=O) and ν(P–O) can be broadened and down-shifted below expected regions. Formation of such hydrogen bond network can be easily recognized in IR spectra as a raised background at about 1000, 1500 and 3000 cm^{-1}. However, the background of the MC4 spectrum does not seem to be raised except the range 1000–1200 cm^{-1}. All modes that include P–O bonds vibrations show some complexity. Thus, they can be successfully extracted from spectra based on quantum-chemical calculations only, as is shown in Tables 3 and 4.

Table 3
Experimental and calculated (B3PW91/6-31G**) frequencies for MC4(0) in cm^{-1}

Experimental frequency	Calculated frequency	Assignment based on PED (%)
1646	1622	ν ring (50)
1636	1567	$\delta(N_1–H_{20})$ (33) + ν ring (32)
1528	1492	ν ring (42) + $\delta(C_6–H_{16})$ (15)
1501	1471	$\delta(C_2–H_{13})$ (16) + ν ring (27) + $\delta(C_3–H_{14})$ (13) + $\delta(C_5–H_{15})$ (10)
1435	1398	$\delta(N_1–H_{20})$ (19) + ν ring (64)
1388		
1359	1367	$\delta(O_8–H_{18})$ (23) + $\nu(C_4–C_7)$ (20) + $\delta(C_7–H_{17})$ (29)
1281	1296	$\delta(C_3–H_{14})$ (17) + $\delta(O_8–H_{18})$ (14) + $\delta(C_5–H_{15})$ (14) + $\delta(C_6–H_{16})$ (14)
1259	1283	$\nu(P_9{=}O_{12})$ (43) + $\nu(P_9{=}O_{11})$ (42)
1239	1239	$\delta(O_8–H_{18})$ (37) + $\delta(C_6–H_{16})$ (16)
1217	1230	$\delta(C_2–H_{13})$ (21) + $\delta(N_1–H_{20})$ (17) + $\delta(O_8–H_{18})$ (16) + $\nu(C_4–C_7)$ (11)
1188	1221	$\delta(C_7–H_{17})$ (35) + $\nu(C_4–C_7)$ (10)
1160	1164	$\delta(C_5–H_{15})$ (19) + $\delta(C_3–H_{14})$ (18) + $\delta(C_2–H_{13})$ (17) + $\nu(C_6–H_{16})$ (13)
1114	1103	$\nu(C_7–O_8)$ (50)
1086	1065	$\nu(P_9{=}O_{11})$ (41) + $\nu(P_9{=}O_{12})$ (29)
1067	1057	$\nu(C_7–O_8)$ (22) + $\nu(N_1–C_2)$ (12) + $\nu(C_5–H_{15})$ (12)
1032		
1005	1026	δ ring (24) + ν ring (31) + $\delta(C_5–H_{15})$ (12)
976	996	$\delta(C_7–H_{17})$ (32) + $\delta(O_{10}–H_{19})$ (13)
	983	$\delta(O_{10}–H_{19})$ (66) + δ ring (11)
	955	δ ring (16) + $\delta(C_7–H_{17})$ (25)
918	944	$\gamma(C_5–H_{15})$ (46) + $\gamma(C_6–H_{16})$ (32)
	921	$\gamma(C_2–H_{13})$ (44) + $\gamma(C_3–H_{14})$ (36)
861	827	$\gamma(C_3–H_{14})$ (27) + $\gamma(C_2–H_{13})$ (23)
840	814	$\nu(C_4–C_7)$ (18) + $\nu(C_4–C_5)$ (13) + $\gamma(C_6–H_{16})$ (11)
	801	$\gamma(C_3–H_{14})$(37) + $\gamma(C_2–H_{13})$ (36) + $\gamma(C_6–H_{16})$ (11)
756	738	$\nu(P_9–O_{10})$ (82)
711	697	τ ring (63) + $\gamma(C_4–C_7)$ (12)
669	659	$\gamma(N_1–H_{20})$ (73)
653	622	δ ring (88)
634	603	τ ring (35) + $\delta(C_7–O_8)$ (29)
578	587	$\nu(C_7–P_9)$ (24) + τ ring (22) + $\delta(C_7–O_8)$ (15) + $\gamma(N_1–H_{20})$ (14)
557	534	$\tau(O_8–H_{18})$ (68) + $\tau(O_{10}–H_{19})$ (17)
478	498	$\delta(P_9{=}O)$ (17) + $\delta(P_9–O_{10})$ (13) + τ ring (10)
465	474	τ ring (11)
440	425	$\delta(P_9{=}O)$ (57) + $\tau(C_7–P_9)$ (10)
420	408	τ ring (30) + $\gamma(C_4–C_7)$ (17) + $\nu(C_7–P_9)$ (12)

The successive proton dissociation shifts the phosphonic group vibrations as a result of change of the P–O bond order. The first phosphonic group deprotonation leads to MC4 zwitteranionic form and is connected with delocalisation of negative charge what causes loss of the nature of the $P_9{=}O_{11}$ double bond. Consequently, the two stretchings of $\nu(P_9{=}O_{11})$ and $\nu(P_9{=}O_{12})$ at 1259 and 1086 cm^{-1} are observed. The P=O mode of this class of compounds was observed and discussed by us earlier; for example, for derivatives of MC4 (*meta*-isomer and carboxylopyridine phosphonic acids). This mode is observed in the 1280–1030 cm^{-1} range [10,11]. As can be expected, the deprotonation of the pyridine ring does not influence significantly (P=O) vibrations [11]. However, MC4(−2) dianion is characterized by three equivalent P–O bonds that are observed at 1123, 1078 and 1069 cm^{-1}.

The ν(P–C) mode is expected in the 700–600 cm^{-1} range and appears at 578 and 581 cm^{-1} for MC4(0) and MC4(−2) forms, respectively.

Quite good agreement between experimental and calculated data indicates that assumed forms of MC4

Table 4
Experimental and calculated (B3PW91/6-31G**) frequencies for MC4(−2) in cm^{-1}

Experimental frequency	Calculated frequency	Assignment based on PED (%)
1634	1586	vring (45)
1601	1491	vring (65) + δring (10)
1554	1464	$\delta(O_8–H_{18})$ (81)
1598	1461	$\delta(C_2–H_{13})$ (18) + $\delta(C_6–H_{16})$ (16) + $\delta(C_3–H_{14})$ (13) + $\nu(C_3–C_4)$ (11) + $\nu(C_4–C_7)$ (10)
1413	1409	vring (56) + $\delta(C_6–H_{16})$ (12) + $\delta(C_2–H_{13})$ (12)
1335	1326	$\delta(C_7–H_{17})$ (50) + $\nu(C_4–C_7)$ (15)
1292	1295	vring (39) + $\delta(C_6–H_{16})$ (18) + $\delta(C_2–H_{13})$ (15)
1241	1265	$\nu(C_4–C_7)$ (15) + $\delta(C_5–H_{15})$ (14) + $\delta(C_4–C_5)$ (12) + $\delta(C_6–C_{16})$ (12)
1227	1218	$\delta(C_7–H_{17})$ (18) + $\nu(C_3–C_4)$ (14) + $\nu(C_4–C_7)$ (12)
1199	1176	$\delta(C_2–H_{13})$ (19) + $\delta(C_3–H_{14})$ (15) + $\delta(C_6–H_{16})$ (13) + $\delta(C_5–H_{15})$ (11) + $\nu(N_1–C_2)$ (10)
1123	1155	$\nu(P_9–O_{12})$ (52) + $\nu(P_9–O_{11})$ (34)
1078	1080	$\nu(C_7–O_8)$ (26) + $\nu(P_9–O_{10})$ (21) + $\nu(P_9–O_{11})$ (12) + $\nu(P_9–O_{11})$ (12)
1069	1060	$\nu(P_9–O_{11})$ (21) + $\nu(C_7–O_8)$ (18) + $\nu(P_9–O_{10})$ (18)
1041	1041	$\nu(C_7–O_8)$ (25) + $\nu(C_3–H_{14})$ (17) + δring (17) + vring (26)
1000	1027	$\delta(C_5–H_{15})$ (35) + vring (24)
965	970	δring (32) + $\delta(C_7–H_{17})$ (14) + $\nu(N_1–C_2)$ (11)
935	933	$\delta(C_7–H_{17})$ (37)
	929	$\gamma(C_2–H_{13})$ (29) + $\gamma(C_6–H_{16})$ (26) + $\gamma(C_5–H_{15})$ (17) + $\gamma(C_3–H_{14})$ (16)
	917	$\gamma(C_6–H_{16})$ (24) + $\gamma(C_2–H_{13})$ (18) + $\gamma(C_5–H_{15})$ (17) + $\gamma(C_3–H_{14})$ (12) + τring (10)
882	894	$\delta(O_8–H_{18})$ (63) + $\nu(P_9–O_{10})$ (13)
866	863	$\nu(P_9–O_{10})$ (37) + $\delta(O_8–H_{18})$ (23) + $\nu(P_9–O_{11})$ (15) + $\nu(P_9–O_{12})$ (12)
835	846	$\gamma(C_5–H_{15})$ (34) + $\gamma(C_3–H_{14})$ (26) + $\gamma(C_6–H_{16})$ (20) + $\gamma(C_2–H_{13})$ (17)
786	809	$\nu(C_4–C_7)$ (14)
757	801	$\gamma(C_3–H_{14})$ (15) + $\gamma(C_2–H_{13})$ (14) + $\gamma(C_5–H_{15})$ (13) + $\gamma(C_6–H_{16})$ (11)
719	723	τring (68) + $\gamma(C_4–C_7)$ (12)
666	653	δring (90)
643	602	δring (26) + $\delta(C_7–O_8)$ (23)
581	587	$\delta(C_7–O_8)$ (27) + $\nu(C_7–P_9)$ (22)
534	529	$\delta(P_9–O)$ (76)
483	499	$\delta(P_9–O_{12})$ (18) + δring (15) + $\gamma(C_4–C_7)$ (15) + $\delta(C_7–O_8)$ (14)
456	447	$\delta(P_9–O)$ (55)
433	433	$\delta(P_9–O)$ (70)

(Fig. 1) used in calculation reflect well structures of MC4 at individual pH range.

4. Summary

Vibrational spectra obtained for the zwitterionic and the dianionic forms of (hydroxypyridin-4-yl-methyl)phosphonic acid are fairly good reproduced by the B3PW91/6-31G** method. There is observed correlation between the consecutive deprotonation of MC4 and the ring aromaticity, which is confirmed by calculated the HOMA index. The aromaticity changes follow with changes of charge distribution estimated by the GAPT analysis.

Acknowledgements

The authors thank Dr. B. Boduszek for supplying (hydroxypyridin-4-yl-methyl)phosphonic acid (MC4) and Dr. A. Wesełucha-Birczyńska for measuring FT-Raman spectra. The authors are grateful to Academic Computer Center ''Cyfronet'' in Kraków for conducting all design calculations.

References

[1] H. Fleisch, Drugs 42 (6) (1991) 919.
[2] B. Boduszek, M. Dyba, M. Jeżowska-Bojczuk, T. Kiss, H. Kozlowski, Chem. Soc., Dalton Trans. (1997) 973.

[3] B. Boduszek, J. Prakt. Chem. 334 (1992) 444.
[4] M. Dyba, M. Jeżowska-Bojczuk, E. Kiss, T. Kiss, H. Kozłowski, Y. Leroux, D. El Manouni, J. Chem. Soc., Dalton Trans. (1996) 973.
[5] M. Dyba, H. Kozłowski, A. Tlalka, Y. Leroux, D. El Manouni, Pol. J. Chem. (1998) 1148.
[6] E. Gumienna-Kontecka, J. Jezierska, M. Lecouvey, Y. Leroux, H. Kozłowski, J. Inorg. Biochem. (2002) 13.
[7] L. Chruściński, P. Młynarz, K. Malinowska, J. Ochocki, B. Boduszek, H. Kozłowski, Inorg. Chem. Acta (2000) 303.
[8] K. Chruszcz, M. Barańska, K. Czarniecki, B. Boduszek, L.M. Proniewicz, J. Mol. Struct. 648 (2003) 215.
[9] K. Chruszcz, M. Barańska, K. Czarniecki, L.M. Proniewicz, J. Mol. Struct. 651C–653C (2003) 729.
[10] M. Barańska, K. Chruszcz, B. Boduszek, L.M. Proniewicz, Vib. Spectr. 31 (2) (2003) 295.
[11] M. Barańska, K. Chruszcz, M. Podkulska, M. Fościak, L.M. Proniewicz, J. Mol. Struct., in press.
[12] K. Chruszcz, M. Barańska, K. Lewiński, L.M. Proniewicz, Vib. Spectr., in press.
[13] B. Boduszek, Tetrahedron 52 (1996) 12483.
[14] B. Boduszek, Phosphorus Sulphur Silicon 113 (1996) 209.
[15] J. Ciosłowski, J. Am. Chem. Soc. 111 (1989) 8333.
[16] T.M. Krygowski, M. Cyrański, Tetrahedron 52 (1996) 10255.
[17] T.M. Krygowski, M. Cyrański, Tetrahedron 52 (1996) 1713.
[18] A.D. Becke, J. Chem. Phys. 98 (1993) 5648.
[19] J.P. Perdew, Y. Wang, Phys. Rev. B 45 (1992) 13244.
[20] J.P. Perdew, J.A. Chevary, S.H. Vosko, K.A. Jackson, M.R. Pederson, D.J. Singh, C. Fiolhais, Phys. Rev. B 46 (1992) 6671.
[21] M.J. Frisch, G.W. Trucks, H.B. Schlegel, G.E. Scuseria, M.A. Robb, J.J.R. Cheeseman, V.G. Zakrzewski, J.A. Montgomery, R.E. Stratmann, J.C. Burant, S. Dapprich, J.M. Millam, A.D. Daniels, K.N. Kudin, M.C. Strain, O. Farkas, J. Tomasi, V. Barone, M. Cossi, R. Cammi, B. Mennucci, C. Pomelli, C. Adamo, S. Cliffird, J. Ochterski, G.A. Petersson, P.Y. Ayala, Q. Cui, K. Morokuma, D.K. Malick, A.D. Rabuck, K. Raghavachari, J.B. Foresman, J. Ciosłowski, J.V. Ortiz, B.B. Stefanov, G. Liu, A. Liashenko, P. Piskorz, I. Komaromi, R. Gomperts, R.L. Martin, D.J. Fox, T. Keith, M.A. Al-Laham, C.Y. Peng, A. Nanayakkara, C. Gonzalez, M. Challacombe, P.M.W. Gill, B.G. Johnson, W. Chen, M.W. Wong, J.L. Andres, M. Head-Gordon, E.S. Replogle, J.A. Pople, Gaussian'98 (Revision A.1), Gaussian Inc., Pittsburgh, PA, 1998.
[22] A.P. Scott, L. Radom, J. Phys. Chem. 100 (1996) 16502.
[23] J.M.L. Martin, C. Van Alsenoy, Gar2ped, University of Antwerp, 1995.
[24] G. Fogarasi, X. Zhou, P.W. Taylor, P. Pulay, J. Am. Chem. Soc. 114 (1992) 8191.
[25] P. Pulay, G. Fogarasi, F. Pang, J.E. Boggs, J. Am. Chem. Soc. 101 (1979) 2550.
[26] P. Flukiner, H.P. Luthi, S. Portman, J. Weber, MOLEKEL 4.2, Swiss Center for Scientific Computing, Manno, Switzerland, 2000–2002.
[27] T.M. Krygowski, J. Chem. Inf. Comput. Sci. 33 (1993) 70.
[28] A. Mrozek, J. Karolak-Wojciechowska, P. Amiel, J. Barbe, J. Mol. Struct. 524 (2000) 151.
[29] J.A. Joule, G.F. Smith, Chemia związków heterocyklicznych, PWN, Warszawa, 1984.
[30] R.S. Mulliken, J. Chem. Phys. 23 (1955) 1833.
[31] R.S. Mulliken, J. Chem. Phys. 36 (1962) 3428.
[32] P.O. Lödwin, J. Chem. Phys. 21 (1955) 374.
[33] A.E. Reed, R.B. Wienstock, F. Weinhold, J. Chem. Phys. 83 (1985) 735.
[34] W.B. Person, J.H. Newton, J. Chem. Phys. 61 (1974) 1040.